energies

MDPI

Article

Life Cycle and Exergoenvironmental Analyses of Ethanol: Performance of a Flex-Fuel Spark-Ignition Engine at Wide-Open Throttle Conditions

Eduardo J. C. Cavalcanti [1,*], Daniel R. S. da Silva [1] and Monica Carvalho [2]

[1] Department of Mechanical Engineering, Federal University of Rio Grande do Norte (UFRN), Natal 59072-970, Brazil; daniel.contadepesquisa@hotmail.com
[2] Department of Renewable Energy Engineering, Federal University of Paraíba (UFPB), João Pessoa 58051-900, Brazil; monica@cear.ufpb.br
* Correspondence: educanti@gmail.com

Abstract: The growth in the number of vehicles circulating has led to a proportional increase in polluting gas emissions. Bioenergy can be used to help meet these increasing energy demands and mitigate environmental impacts. This work verified the effect of the content of ethanol on the exergy and exergoenvironmental analyses of a spark-ignition engine. Different gasoline–ethanol mixtures were tested along with hydrous ethanol (4.6% water by volume). The thermodynamic data refer to wide-open throttle conditions and variable engine speeds. The life cycle assessment methodology quantified the environmental impacts associated with equipment and fuel using the Eco-indicator 99 method. Pollutants emitted during combustion were measured and included in the environmental assessment (nitrogen oxides, carbon monoxide, and dioxide). Hydrous ethanol at 1500 rpm presented the highest energy efficiency. The effects of the environmental impact rate of pollutant formation and exergy efficiency were significantly higher than the environmental impact rate of fuel. The lowest specific environmental impact of the product (brake power) was 24.39 mPt/MJ, obtained with the fuel blend with 50% ethanol at 2500 rpm. The combined evaluation of the exergoenvironmental factor and the relative difference in environmental impact indicated the optimization priorities and where improvements should be directed.

Keywords: ethanol; life cycle assessment; internal combustion engine; gasoline; ethanol; exergoenvironmental analysis

Citation: Cavalcanti, E.J.C.; da Silva, D.R.S.; Carvalho, M. Life Cycle and Exergoenvironmental Analyses of Ethanol: Performance of a Flex-Fuel Spark-Ignition Engine at Wide-Open Throttle Conditions. *Energies* **2022**, *15*, 1422. https://doi.org/10.3390/en15041422

Academic Editors: Xiaolin Wang and Firoz Alam

Received: 17 January 2022
Accepted: 2 February 2022
Published: 15 February 2022

1. Introduction

The ever-increasing vehicle fleet has led to higher demand and depletion of fossil fuels and has increased the emission of pollutants. Internal combustion engines (ICE) are the central propulsion systems in road transport [1], and estimates indicate that by 2040, there will be more than 1.7 billion vehicles [2]. According to the International Organization of Motor Vehicle Manufacturers [3], road transport is currently responsible for approximately 16% of global carbon emissions. Despite representing a smaller share compared with electricity-related emissions, the carbon emissions associated with fuel oil consumption in the transport sector have been growing continuously [4], increasing from 6,102 Mt in 2010 to 8040 Mt in 2017.

The combustion of fossil fuels has enhanced climate change and global warming [5], and the consumption of these fuels, such as gasoline and diesel, represents a considerable share of primary energy consumption in the world. One of the alternatives studied to reduce ICE emissions is the use of alternative fuels, such as biofuels [6]. The global biofuel market is dominated by ethanol, with more than 70% of the market, of which Brazil is the largest producer, followed by the United States [7]. Ethanol (C_2H_5OH) is a liquid, transparent, neutral, colorless, flammable, volatile, and oxygenated hydrocarbon, produced

from biological material by fermentation processes; in Brazil, it is produced mainly from sugarcane.

Ethanol has favorable properties compared with gasoline (but also has drawbacks) [6–10]. Its higher octane number enables higher compression rates in combustion, leading to higher efficiency and power. Its high heat of vaporization causes a reduction in the maximum temperature inside the cylinder, favoring higher volumetric compression rates. Higher combustion temperatures are also obtained for ethanol due to its oxygen content. However, its lower heating value (LHV) is about one-third of gasoline's LHV; therefore, more fuel is required to achieve the same power. Moreover, its low vapor pressure can cause cold starting issues, and the polarity and its hydrophilic nature can cause corrosion in ferrous components.

In the search to reduce the levels of environmental pollution, studies have been carried out focusing on the use of biofuels, either pure or mixed with conventional fuels, such as the use of gasoline–ethanol blends. The addition of up to 10% ethanol results in a decrease in carbon monoxide (CO) [11]. He et al. [12] indicated that in addition to reducing CO, there is also a reduction in NOx in emissions and an increase in the number of octane when a gasoline–ethanol blend is used. Zhao et al. [13] added ethanol to gasoline (20% by volume) to increase antiknock performance, resulting in higher combustion efficiency and 5% lower fuel consumption than gasoline in stoichiometric conditions. The effects of C3 and C4 alcohols in gasoline in spark-ignition (SI) engines were investigated by [7] regarding the characteristics of emissions and combustion, concluding that the addition of alcohol potentially reduces soot, unburned hydrocarbons (UHC), and CO emissions while increasing thermal efficiency. When a SI engine was tested at various speeds with gasoline–ethanol blends (0–5% ethanol), better engine performance was obtained with the addition of ethanol [14]. Ethanol–gasoline mixtures were used in the SI engine tested by Iodice et al. [15], who obtained lower HC and CO emissions with the addition of ethanol. A similar study was carried out by Chen et al. [16], who obtained significant decreases in HC and CO emissions with 20–30% ethanol content.

There are also studies focusing on the performance of ethanol-fueled engines. Costa et al. [17] investigated the combustion of hydrous ethanol in a SI engine, improving fuel consumption and conversion efficiency for a 1.4 theoretical air ratio, with reductions in NOx, total hydrocarbons (THC), and CO emissions. Lanzanova et al. [18] evaluated the operation of a SI engine with direct injection of ethanol mixed with water (5–20% by volume), in which the higher content of water affected the rate of heat released, increasing the duration of combustion, reducing NOx emissions at the cost of higher UHC emissions. Costa et al. [19] developed a methodology to design and experimentally characterize a homogenous pre-chamber torch ignition system, fed with hydrated ethanol (6 to 7% water by weight) with excess air for an SI engine. Fuel conversion efficiency increased by 5.4%, with specific consumption decreasing by 22%, achieving a decrease in NOx emissions. Ambrós et al. [20] developed a mathematical model to predict the performance of hydrous ethanol (10–40% ethanol by volume) in an ICE, demonstrating that fuel with 30% water showed better performance than commercial ethanol with 5% water by volume.

Most performance analyses are based on the First Law of Thermodynamics, in which the concepts of mass and energy balances are applied. Going a step further, exergy assessments are carried out to fill this gap. SI engines [21–24] and compression ignition engines [25–28] have been the focus of exergy assessments, where irreversibilities are quantified (mainly due to combustion) along with exergy losses associated with heat transfer to the environment and exhaust gases [23,29–32]. Exergy can also be used within a sustainability perspective to determine the environmental impacts of energy conversion systems. In this sense, exergoenvironmental analysis [33] combines exergy analysis with the Life Cycle Assessment (LCA) methodology to quantify the environmental damage associated with manufacturing the engine and producing the fuels and helps identify where the environmental impacts are produced and how these are distributed throughout the system. The LCA is a state-of-the-art methodology, internationally consolidated, that

quantifies the potential environmental impacts associated with a process or component [34]. Exergoenvironmental assessments can identify the main sources of environmental impacts in energy conversion systems and how these are allocated to internal flows and products, guiding the decision-making process towards environmental sustainability. Exergoenvironmental and exergoeconomic assessments were developed for a compression ignition engine powered with biodiesel–diesel blends, where the environmental impacts decreased with the addition of biodiesel [35]. The addition of 1-heptanol to diesel was studied by [36] for compression-ignition engine applications, with the development of energy, exergy, exergoeconomic, enviroeconomic, and sustainability analyses.

Recognizing the knowledge gap regarding the introduction of bioenergy in current fossil-based energy schemes, this work is based on experimental data obtained a priori for engine operation at wide-open throttle conditions and varied engine speeds. The objective was to verify the impacts of different ethanol contents on the exergy and exergoenvironmental assessments of a flex-fuel SI engine. Different gasoline–ethanol mixtures (25%, 50%, and 75% ethanol by volume) are tested, along with hydrous ethanol (4.6% water by volume, in line with Brazilian standards). Emissions were taken into account in the combustion step of the assessment. The environmental impacts of manufacturing the engine and producing the fuels were considered, yielding specific environmental impacts (per unit of exergy). To this end, LCAs were developed and are presented in detail herein.

The main contribution of this study is to verify the behavior of the specific environmental impact associated with the production of power by an ICE as the proportion of ethanol is increased in fuel mixtures.

2. Materials and Methods

2.1. Engine and Fuel Specifications

The theoretical assessment carried out herein was based on data from [37] on a flex-fuel SI engine, which was analyzed via a dynamometer bench test. Table 1 shows the engine's specifications as presented by [37], and Table 2 shows the properties of pure gasoline and ethanol as presented by [8].

Table 1. Engine specifications [37].

Engine	GM Powertrain- Econoflex 8V
Cylinders	4 in line
Stroke volume	1389 (cm^3)
Compression ratio	12.4:1
Max. power: gasohol/ethanol	72.8/77.2 (kW)
Max. torque: gasohol/ethanol	129/131 (Nm)
Idle/max. speed	800/6000 (rpm)
Weight	103 (kg)

The description of the tests and experimental procedures followed Carvalho [37], who used a Schenck model D-210E (maximum torque capacity of 600 Nm and 200 kW power). Fuel consumption was verified using the gravimetric method with a 3-decimal resolution scale (Toledo model). A Pitot tube-type anemometer was utilized to measure the flow of intake air, and a K-type temperature sensor was placed in the exhaust pipe to measure the temperature of the exhaust gases. A Telegan Tempest 50 gas analyzer determined the composition of the exhaust gases, which provided readings of NOx, CO, CO_2, and O_2. After the engine reached its working temperature, operation data at wide-open throttle (WOT) conditions were obtained for engine speeds of 1500, 2000, and 2500 rpm. The temperature and pressure of the inlet air and fuel were considered as ambient conditions: 25 °C and 101.15 kPa. The pressure of exhaust gases was considered to be 101.15 kPa.

Table 2. Properties of fuels [8].

Properties	Gasoline	Ethanol
Chemical formula	C_5 to C_{12}	C_2H_5OH
Density (kg/m^3)	760	785
Molecular weight (kg/kmol)	114.15	46.07
Composition, weight %	-	-
Carbon	87.4	52.2
Hydrogen	12.6	13.1
Oxygen	0	34.7
Adiabatic flame temperature (K)	2270	1920
Higher heating value (MJ/kg)	47.3	29.7
Lower calorific value (MJ/kg)	44.0	26.9
Stoichiometric air fuel ratio	14.2–15.1	8.97
Research octane number	95	108
Enthalpy of formation (kJ/kmol)	-	-
(a) Liquid	−259,280	−224,100
(b) Gas	−277,000	−234,600

The assessment carried out herein considers gasohol E25 (25% anhydrous ethanol, by volume, in gasoline), a gasohol E50 mixture (50% anhydrous ethanol, by volume, in gasoline), a gasohol E75 mixture (75% anhydrous ethanol, by volume, in gasoline), and hydrous ethanol E100 (4.6% water by volume).

2.2. Combustion and Energy Analysis

The combustion that occurred in the engine is shown by Equations (1) and (2), which describe the burning molar percentage of each fuel with moist atmospheric air. The volumetric composition of the moist atmospheric air is 20.59% O_2, 77.48% N_2, 1.9% $H_2O(g)$, and 0.03% CO_2. Equation (1) describes the combustion of a mixture based on the molar percentage of gasoline (y_{gas}) and ethanol (y_{eth}) according to their volumetric proportion. The chemical formula of gasoline, considering the molecular weight and the mass ratios of carbon and hydrogen as shown in Table 2, is $C_{8.31}$ $H_{14.27}$. Equation (2) describes the combustion of hydrous ethanol (E100), in which a molar portion of the fuel is composed of water in a liquid state mixed with ethanol (C_2H_5OH).

$$\left[y_{gas} \cdot C_{8.31}H_{14.27} + y_{eth} \cdot C_2H_5OH\right] + \lambda \cdot X_{O2}\left[O_2 + 3.763 \cdot N_2 + 0.092 \cdot H_2O_{(g)} + 0.0015 \cdot CO_2\right] \rightarrow \beta_1 \cdot CO_2 + \beta_2 \cdot H_2O + \beta_3 \cdot O_2 + \beta_4 \cdot N_2 + \beta_5 \cdot NO + \beta_6 \cdot CO \quad (1)$$

$$\left[0.86 \cdot C_2H_5OH + 0.14 \cdot H_2O_{(L)}\right] + \lambda \cdot X_{O2}\left[O_2 + 3.763 \cdot N_2 + 0.092 \cdot H_2O_{(g)} + 0.0015 \cdot CO_2\right] \rightarrow \beta_1 \cdot CO_2 + \beta_2 \cdot H_2O + \beta_3 \cdot O_2 + \beta_4 \cdot N_2 + \beta_5 \cdot NO + \beta_6 \cdot CO \quad (2)$$

where λ is the theoretical amount of air, X_{O2} is the minimum consumption of oxygen moles per fuel mole for complete combustion in a stoichiometric reaction without excess air, and β represents the stoichiometric coefficients of gaseous combustion products evaluated by chemical species balance, which are the input data related to specific pollutant gas emissions. The conversion of specific pollutants (g/kWh) to stoichiometric coefficients β can be found in Cavalcanti [38]. The unburned hydrocarbon in exhaust gases was not considered. For each fuel mixture, the molar percentages in Equation (1) were: E25, 0.54 gasoline/0.46 ethanol; E50, 0.28 gasoline/0.72 ethanol; and E75, 0.12 gasoline/0.88 ethanol.

The control volume considered for the energy analysis included the engine (Figure 1). Steady-state conditions were assumed.

Figure 1. Energy balance in the SI engine.

The mass flows of the fuel and atmospheric air used for combustion were measured and considered at ambient temperatures and pressures, at Points 1 and 2, respectively. The temperature of the exhaust gases was measured and considered to be released at ambient pressure at Point 3. The engine power was measured using the dynamometer at Point 4. The heat losses, represented by Point 5, include losses within the coolant and lubricating oil, and heat losses to the environment.

The First Law of Thermodynamics for systems and reagents [39] was used to carry out the energy balance and to quantify the heat losses to the environment, as shown in Equation (3).

$$\dot{Q}_{CV} + \sum_R n_{in}\left(\overline{h}_f^0 + \Delta\overline{h}\right)_{in}.\dot{n}_{fuel} = \sum_P n_{out}\left(\overline{h}_f^0 + \Delta\overline{h}\right)_{out}.\dot{n}_{fuel} + \dot{W}_{CV} \quad (3)$$

where n is the number of moles of the reactant and products in the combustion reaction per kmol unit of fuel, $\overline{h}_f^0$ is the enthalpy of the formation of each substance, and $\Delta\overline{h}$ is the variation in the formation enthalpy concerning the dead state. The subscripts R and P correspond to the reagent and the product, respectively. The formation enthalpy values for gasoline and ethanol follow those in Table 2. $\dot{n}_{fuel}$ is the flow rate of fuel (in moles), used to convert the enthalpy on a molar basis into kW. The units of $n\cdot\left(\overline{h}_f^0 + \Delta\overline{h}\right)\dot{n}_{fuel}$ are $kmol/kmol_{fuel}.(kJ/kmol).kmol_{fuel}/s = kJ/s$.

2.3. Exergoenvironmental Analysis

The exergoenvironmental methodology was developed by Meyer et al. [33], who indicated that understanding the formation of environmental impacts is essential for improving the ecological performance of energy conversion systems. The method identifies the sources of environmental impact and tracks the formation of pollutants throughout the system.

Exergoenvironmental analysis consists of three steps:

(i) Exergy analysis of the energy conversion system;
(ii) LCA of the energy conversion equipment and of all associated input and output energy streams;
(iii) Allocation of environmental information obtained via the LCA to all exergy flows of the system.

2.3.1. Exergy Analysis

The exergy analysis was based on the SPecific Exergy COsting methodology (SPECO), as reported by Lazzaretto and Tsatsaronis [40]. SPECO defines and calculates exergy efficiencies related to exergy costs in thermal systems, based on the records of all additions and removals of exergy flows, establishing a direct link between the definitions of fuel ($\dot{E}_F$) and the product ($\dot{E}_P$) for a component. The balance also considers losses of exergy due to

heat transfers ($\dot{E}_L$). The exergy balance followed Bejan, Tsatsaronis, and Moran [41], as described in Equation (4).

$$\dot{E}_F = \dot{E}_P + \dot{E}_{Loss} + \dot{E}_D \quad (4)$$

where $\dot{E}_D$ is the rate of exergy destruction. The exergy rate of the product ($\dot{E}_P$) is the axis power measured at Point 4 ($\dot{E}_P = \dot{E}_4$). The exergy rate of the ICE fuel ($\dot{E}_F$) is $\dot{E}_1 + \dot{E}_2 - \dot{E}_3$. The exergy rate of atmospheric air is zero ($\dot{E}_1 = 0$). The exergy rate of the liquid fuel injected into the engine ($\dot{E}_2$) is calculated by multiplying the flow of fuel by its chemical exergy (e^{CH}), calculated according to Appendix C of Kotas [42] for liquid fuels, as shown in Equations (5) and (6).

$$e^{CH} = \beta_F \cdot LHV \quad (5)$$

$$\beta_F = 1.0401 + 0.1728 \cdot \left(\frac{H}{C}\right) + 0.0432 \cdot \left(\frac{O}{C}\right) \quad (6)$$

where β_F is the ratio of chemical exergy to net (low) heat value (LHV). C, H, and O are the mass fractions of carbon, hydrogen, and oxygen contained in the fuel, respectively. The accuracy of this expression is estimated to be ± 0.38%.

The chemical exergy of a gaseous mixture can be calculated by Equation (7) [41].

$$e_g^{CH} = \sum_i y_i \cdot e_0^{CH} + R \cdot T_0 \cdot \left(\sum_i y_i \cdot \ln(y_i)\right) \quad (7)$$

where y_i is the molar fraction of the mixture component, R is the universal gas constant (8.3145 kJ/(kmol.K)), and e_0^{CH} is the standard chemical exergy of each substance [43].

The rate of loss of exergy due to heat transfer ($\dot{E}_L$) is calculated according to Equation (8) [41].

$$\dot{E}_L = \dot{Q}_{CV} \cdot \left(1 - \frac{T_0}{T_{surf}}\right) \quad (8)$$

where $\dot{Q}_{CV}$ is the heat rate, T_0 is the ambient temperature [K], and T_{surf} is the surface temperature of the engine, which can also be considered the thermodynamic average temperature (in Kelvin).

The exergy efficiency (ε) for the engine according to the SPECO methodology [40] is calculated by Equation (9).

$$\varepsilon = \frac{\dot{E}_P}{\dot{E}_F} \quad (9)$$

2.3.2. Life Cycle Assessment (LCA)

LCA has been standardized by the International Organization for Standardization (ISO) in its standards ISO 14,040 [44] and ISO 14,044 [45], and enables the assessment of the environmental impacts associated with all the stages of a product (or process). The environmental impact assessment method selected herein was the Eco-indicator 99 (EI99) [46] with hierarchical (H) perspective and average (A) weighting factors, which include damages to human health, ecosystem quality, and the use of resources. EI99 includes normalization and weighting steps in the LCA, and assigns a single score to each product or process, calculated on the basis of the relative environmental impact. The score is represented in points, in which each point represents the annual environmental load (i.e., overall production/consumption undertakings in the economy) of an average European citizen [47].

The LCAs of gasoline and ethanol were developed with SimaPro 9.0.0.49 [48] using the database Ecoinvent [46] and the EI99 method [49].

The process for gasoline considered the production of unleaded gasoline at an oil refinery. Operation of storage tanks and refinery facilities was considered, along with transportation of the product from the refinery to the end-user. Operation of storage tanks and petrol stations was included, as well as emissions from evaporation and treatment of effluents.

For ethanol, the process was modeled with ethanol production from sugarcane in Northeast Brazil. This dataset included sugarcane production, transportation to the refinery (in 32-tonne trucks), and its processing into ethanol (95% w/w), bagasse (79% dry matter, excess), and vinasse. Although the refinery can produce sugar and ethanol, sugar has not been produced because of the higher price of ethanol. The system boundary is at the refinery. Treatment of waste effluents was not included (most wastewater is spread over the fields nearby).

Sugarcane was considered as 94% sugarcane stalks, 5% vegetable matter (straw), and 1% mineral (dirt) impurities (yield, inputs, and emissions are related to the average considering the varieties Romeu e Julieta, Treminhão, and Rodotrem). The dataset represented the production of 1 kg of sugarcane (fresh matter). Production encompassed one harvest of plant cane and four harvests of ratoon cane (with declining yields from year to year). Inputs of mineral fertilizers were included, along with transportation of fertilizers, lime, and gypsum to the field. No input of seedlings was considered (sugarcane used as seedlings was considered by reducing sugarcane yield). All machine operations were included, considering 40% mechanized planting and 56% mechanical harvesting (typical conditions for Northeast Brazil, due to the rugged landscape and availability of labor). Infrastructure for machinery storage and maintenance was included in the dataset of these operations.

The environmental impact related to the SI engine was determined from its material composition and is shown in Table 3 [35,50].

Table 3. Environmental impacts of the engine (construction phase).

Material	Weight Composition (%)	Specific Impact (mPt/kg)	Overall Impact (mPt/kg)
Steel	18.52	86	15.93
Iron	60.60	240	145.43
Aluminum	19.76	780	154.16
Polypropylene	0.75	330	2.46
Rubber	0.37	360	1.34
Total	100.00		319.32

2.3.3. Exergoenvironmental Assessment

The exergoenvironmental assessment allocated environmental impacts to the respective k-th exergy flows [33], according to Equation (10).

$$\dot{B}_K = b_K \cdot \dot{E}_K \quad (10)$$

where $\dot{B}_k$ is the rate of environmental impact, in points per unit of time (mPt/s); b_k is the specific environmental impact (per unit of exergy) of the same flow (mPt/GJ); and $\dot{E}_k$ is the exergy rate of the corresponding flow.

The environmental impact rates associated with exergy loss rates ($\dot{E}_L$) and work produced ($\dot{E}_P$) are described by Equation (11) [33,41].

$$\dot{B}_L = b_F \cdot \dot{E}_L \quad (11)$$

where $\dot{B}_L$ is the environmental impact rate of loss of exergy (mPt/s), b_F is the specific environmental impact (per unit of exergy) of the fuel for the component (mPt/kJ), and $b_F = (\dot{B}_2 - \dot{B}_3)/(\dot{E}_2 - \dot{E}_3)$. Based on the fuel principle (F), the specific environmental impacts related to the exergy rates of the engine fuel ($\dot{E}_F$) are equal, and thus $b_2 = b_3$.

Equation (12) shows the environmental impact rate of the product:

$$\dot{B}_P = b_P \cdot \dot{E}_P \quad (12)$$

where $\dot{B}_P$ is the environmental impact rate of the product, which is the brake power (mPt/s), and b_P is the specific environmental impact (per unit of exergy) of the brake power (mPt/kJ). The environmental impact rates associated with the formation of pollutants ($\dot{B}^{PF}$) is calculated by Equation (13).

$$\dot{B}_{PF} = \sum b_i^{PF} \cdot \left(\dot{m}_{i,out} - \dot{m}_{i,in}\right) \quad (13)$$

where $\dot{m}_{i,out}$ and $\dot{m}_{i,in}$ are the mass flows of pollutants that exit and enter the engine, respectively; b_i^{PF} is the specific environmental impact (per unit mass) of the corresponding type of polluting gas. The environmental impacts of each polluting gas produced by the combustion considered in Equations (1) and (2) are 8.36 mPt/kg for CO, 5.45 mPt/kg for CO_2, and 4217.74 mPt/kg for NO [46].

The exergoenvironmental balance, described by Equation (14), encompasses the specific environmental impacts of the input associated with the respective exergy flows, plus the environmental impact rate related to the engine ($\dot{Y}$) (considering a lifetime of 20 years with 2200 operation hours per year.). This is equal to the sum of the specific environmental impacts of the associated output to all respective flows of exergy [41]. Equation (14) aims to determine the environmental impact rates related to the engine's product, in this case, the brake power.

$$\dot{B}_F + \dot{Y} + \dot{B}^{PF} = \dot{B}_P + \dot{B}_L \quad (14)$$

The environmental impacts per unit of exergy of the engine's product consider reallocation of the environmental losses associated with the rate of heat losses [33], shown in Equation (15).

$$b_{P,f} = \left(\frac{\dot{B}_P + \dot{B}_L}{\dot{E}_P}\right) \quad (15)$$

where $b_{P,f}$ is the environmental impact rate per unit of exergy of the brake power produced by the engine (mPt/GJ).

The total environmental impact rate ($\dot{B}_{Tot}$) is therefore the sum of the environmental impacts [33], as given by Equation (16).

$$\dot{B}_{Tot} = \dot{B}_L + \dot{Y} + \dot{B}^{PF} + \dot{B}_D \quad (16)$$

The environmental impact rate related to the destruction of exergy ($\dot{B}_D$) is $\dot{B}_D = b_F \cdot \dot{E}_D$.

Considering the environmental impacts produced by the engine, it is possible to determine the contribution of each environmental impact (y_i^*) to the overall environmental impacts ($\dot{B}_{Tot}$), according to Equation (17).

$$y_i^* = \left(\frac{\dot{y}_i}{\dot{B}_{Tot}}\right) \cdot 100\% \quad (17)$$

The relative difference (r_b) accounts for the average environmental impacts rate per exergy unit of the product (b_P) and of the fuel (b_F) of a component, and indicates the potential for reducing the environmental impact with less effort; r_b represents the environmental quality of an element, as given by Equation (18) [33].

$$r_b = \left(\frac{b_P - b_F}{b_F}\right) \quad (18)$$

The exergoenvironmental factor (f_b) assesses the relative contribution of the environmental impact related to the component ($\dot{Y}$) concerning the sum of the environmental impacts [33], considering the formation of pollutants, as presented by Equation (19):

$$f_b = \left(\frac{\dot{Y} + \dot{B}^{PF}}{\dot{B}_{Tot}} \right) \quad (19)$$

A low value of f_b indicates that the rate of exergy destruction is dominant in relation to the environmental impact rate associated with the component. A component with a low f_b value should improve its efficiency to reduce the exergy destruction rate, thus improving its environmental performance.

3. Results

Regarding combustion, gasoline was evaluated using the carbon and hydrogen mass composition and by considering its molar mass, resulting in $C_{8.31}H_{14.27}$ = 12.011 × 8.31 + 1.008 × 14.27 = 114.15 kg/kmol.

The stoichiometric air–fuel ratio (mass base) was calculated for the fuel mixtures E25, E50, and E75, resulting in 13.09, 11.72, and 10.38, respectively. For ethanol, the stoichiometric air–fuel ratio (mass base) was 8.53.

With an increase in ethanol, the stoichiometric requirements reduced, as ethanol is an oxygenated fuel and already has oxygen molecules in its composition.

Table 4 shows the data used in the models and the results of the combustion balance calculation. The mass fuel flow ($\dot{m}_F$), mass airflow ($\dot{m}_{air}$), and exhaust gas temperature (T_g) follow Carvalho [37]. The pollutants and lambda factor (λ) were evaluated using the stoichiometric balance of the combustion equation, Equations (1) and (2).

Table 4. Combustion analysis and thermodynamic data.

Speed	Fuel	λ	CO_2 (kg/ kg fuel)	CO (kg/ kg fuel)	NO_x (kg/ kg fuel)	$\dot{m}_F$ (kg/s) [37]	$\dot{m}_{air}$ (kg/s) [37]	T_g (°C) [37]
1500	E25	1.121	2.726	0.0933	0.03740	0.00128	0.01883	630
	E50	1.138	2.459	0.0559	0.04428	0.00130	0.01734	616
	E75	1.123	2.130	0.0618	0.03264	0.00152	0.01769	604
	E100	1.159	1.665	0.0865	0.01931	0.00178	0.01761	550
2000	E25	1.131	2.827	0.0287	0.05640	0.00158	0.02344	717
	E50	1.138	2.494	0.0336	0.04897	0.00177	0.02356	681
	E75	1.113	2.176	0.0324	0.03765	0.00190	0.02196	677
	E100	1.138	1.704	0.0617	0.02663	0.00247	0.02392	618
2500	E25	1.049	2.513	0.2284	0.00780	0.00247	0.03387	670
	E50	1.047	2.249	0.1898	0.00620	0.00265	0.03250	669
	E75	1.033	1.959	0.1707	0.00614	0.00303	0.03252	656
	E100	1.075	1.566	0.1493	0.00341	0.00370	0.03392	615

λ is the ratio between the actual air–fuel ratio (measured experimentally) and the stoichiometric air–fuel ratio. An engine operating with a higher ethanol content increases its mass flow. Consequently, with a reduction in the volume of gasoline, the temperature of the exhaust gases was lower. CO_2 emissions decreased with an increase in ethanol at all speeds. For CO, at 1500 rpm, the emissions reduced by almost half from E25 to E50, but increased for E75 and E100. For 2000 rpm, CO emissions increased from E25 to E50, but then decreased for E75 and increased significantly for E100. For NOx emissions at 1500 rpm, there was an increase from E25 to E50, but then a progressive decrease for E75 and E100. At 2000 and 2500 rpm, NOx emissions progressively decreased with the content

of ethanol. Figure 2 shows the variation in emissions per mass of fuel with the different fuels and engine speeds tested.

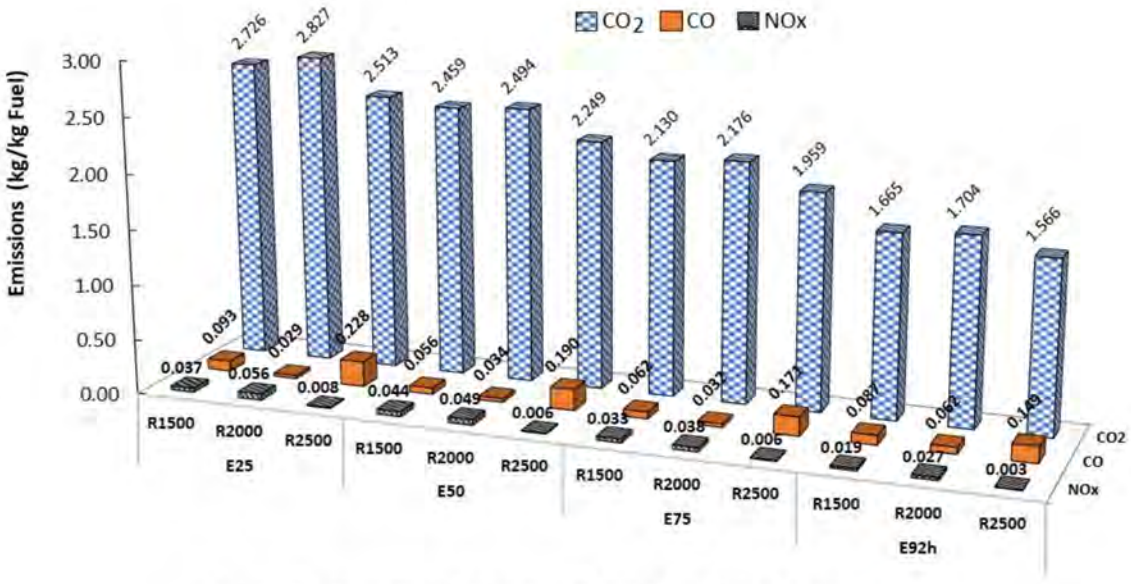

Figure 2. Emissions of pollutants vs. fuels and engine speeds.

Figure 3 shows the variation in energy efficiency with the different fuels and engine speeds tested.

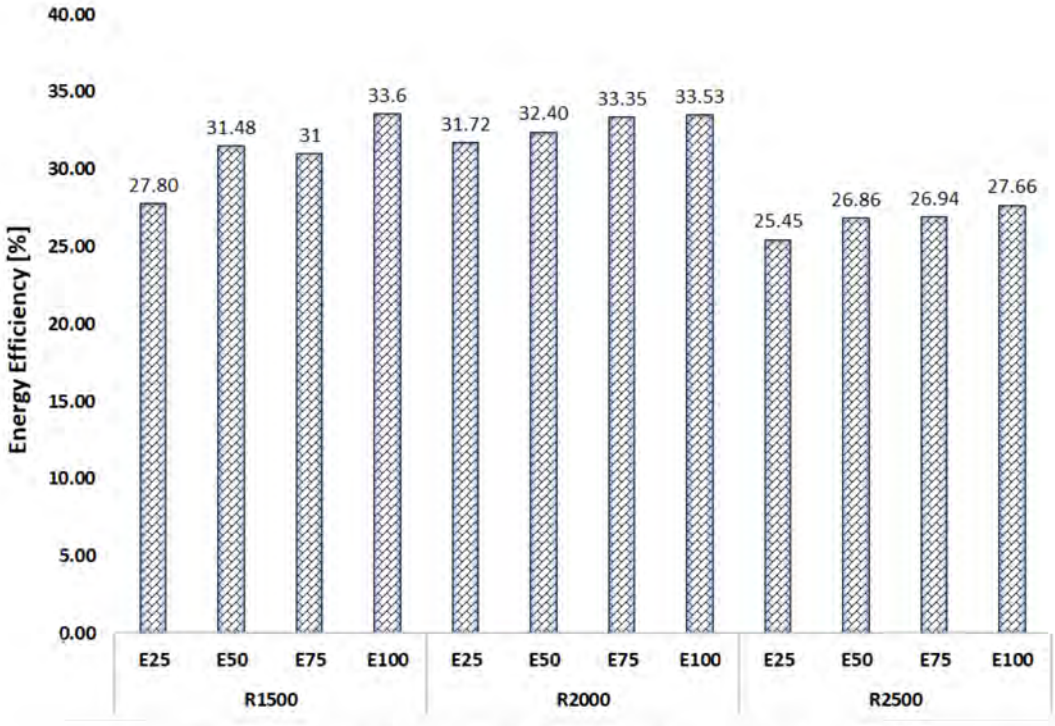

Figure 3. Energy efficiency vs. fuels and engine speeds tested.

From Figure 3, it can be seen that as the content of ethanol increased, the energy efficiency also increased. The maximum energy efficiency values were obtained at 2000 rpm, followed by 1500 rpm and 2500 rpm.

3.1. Life Cycle Assessment

The environmental impact associated with the production of 1 kg of ethanol is 0.214 Pt, of which 87.27% are due to sugarcane cultivation; 0.102 Pt relates to damage to human health, 0.102 Pt to damage to ecosystems, and 0.010 Pt is due to the use of resources. Land use contributed significantly to the overall single score within the ecosystem damage category, along with the emissions into water and soil, mostly related to pesticides and fertilizers.

For gasoline, the environmental impact of 1 kg of fuel is 0.264 Pt, of which 0.045 Pt corresponds to damage to human health, 0.007 Pt to ecosystems, and 0.212 Pt to resources. Of the overall impact, gasoline production itself accounts for 0.235 Pt, with the majority of the remainder associated with pipelines and transportation. The use of non-renewable energy (damage to resources) contributes the most to gasoline's single score.

Table 5 shows the composition and environmental impacts of the fuels used here. It must be highlighted that although the environmental impacts obtained for ethanol and gasoline (0.214 and 0.264 Pt/kg) do not seem too far apart, these values do not include combustion. Combustion is addressed separately within the exergoenvironmental analysis.

Table 5. Composition and environmental impacts of the gasoline–ethanol mixtures.

Fuel	Overall Impact (Pt/kg)
E25	0.251
E50	0.239
E75	0.226
E100	0.214

3.2. Exergy Analysis

Table 6 shows the results of the exergy analysis for each fuel, showing the related exergy rates: fuel ($\dot{E}_2$), exhaust gases ($\dot{E}_3$), heat losses ($\dot{E}_5$), and brake power ($\dot{E}_4$). These flows have been shown in Figure 1.

The fuel exergy rate ($\dot{E}_F$) of the engine combines the exergy rate at Point 2 (the fuel inlet) minus the exergy rate of the exhaust gases at Point 3, according to the SPECO methodology. The exergy rates at Point 2 only represent chemical exergy. There were no clear trends observed for variations in $\dot{E}_2$ with speed or ethanol content.

The exergy rate of the exhaust gases ($\dot{E}_3$) depends on the mass flow of gases and the temperature at the outlet. With an increase in ethanol content, there was a reduction in the temperature of the gases (Table 4), but there was no direct proportionality to the exergy rate of gases ($\dot{E}_3$). $\dot{E}_3$ followed the behavior of $\dot{E}_2$.

The exergy rate of the product ($\dot{E}_P$) represents the brake power produced by the engine at Point 4, according to Figure 1, which presented a progressive increase with speed and ethanol content.

The rate of exergy destroyed ($\dot{E}_D$) was calculated by the exergy balance (Equation (4)), which presented a slight reduction as the concentration increased. The fuel exergy rate ($\dot{E}_F$) is a result of the chemical exergy of the fuel and its mass flow. As the ethanol content increased, the chemical exergy of the fuel reduced and its mass flow increased. The behavior of $\dot{E}_F$ follows $\dot{E}_2$.

The rate of exergy losses associated with heat transfer ($\dot{E}_5$) is a function of the rate of heat loss and the surface temperature of the engine, according to Equation (8).

The exergy efficiency was estimated by Equation (9). The ethanol content seemed to improve the exergy efficiency. The highest exergy efficiency at 1500, 2000 and 2500 rpm was for hydrous ethanol (E100), and the 75% and 50% ethanol blends (E75 and E50).

Table 6. Exergy analysis results.

Speed	Fuel	$\dot{E}_2$ (kW)	$\dot{E}_3$ (kW)	$\dot{E}_4$ (kW)	$\dot{E}_5$ (kW)	$\dot{E}_P$ (kW)	$\dot{E}_F$ (kW)	$\dot{E}_D$ (kW)	$\dot{E}_L$ (kW)	ε (%)
R1500	E25	54.58	9.175	14.14	14.96	14.14	45.41	16.31	14.96	31.14
	E50	49.72	8.011	14.45	13.09	14.45	41.71	14.17	13.09	34.64
	E75	51.65	8.314	14.61	14.26	14.61	43.34	14.47	14.26	33.71
	E100	50.22	8.091	15.17	13.24	15.17	42.13	13.72	13.24	36.01
R2000	E25	67.32	12.44	19.90	16.21	19.90	54.88	18.77	16.21	36.26
	E50	67.58	11.97	20.21	16.84	20.21	55.61	18.56	16.84	36.34
	E75	64.71	11.40	19.69	16.53	19.69	53.31	17.09	16.53	36.93
	E100	69.46	12.10	20.94	18.11	20.94	57.36	18.31	18.11	36.51
R2500	E25	104.9	21.01	24.87	28.30	24.87	83.89	30.72	28.30	29.65
	E50	101.4	20.08	25.13	27.46	25.13	81.32	28.73	27.46	30.90
	E75	103.3	20.23	25.39	29.11	25.39	83.07	28.57	29.11	30.56
	E100	104.2	20.20	25.92	29.50	25.92	84.00	28.58	29.50	30.86

3.3. Exergoenvironmental Analysis

Table 7 shows the results of the exergoenvironmental balance calculation. The values of the specific environmental impacts were calculated: fuel (b2), exhaust gases (b3), brake power (b4), and exergy losses (b5).

Table 7. Exergoenvironmental results.

Speed	Fuel	b_2 (mPt/MJ)	b_3 (mPt/MJ)	b_4 (mPt/MJ)	b_5 (mPt/MJ)	$\dot{B}_P$ (mPt/s)	$\dot{B}_F$ (mPt/s)	$\dot{B}_L$ (mPt/s)	$\dot{B}_D$ (mPt/s)	$\dot{B}^{PF}$ (mPt/s)
1500	E25	5.908	5.908	28.49	5.908	0.403	0.268	0.088	0.096	0.223
	E50	6.237	6.237	30.41	6.237	0.439	0.260	0.082	0.088	0.261
	E75	6.643	6.643	28.78	6.643	0.421	0.288	0.095	0.096	0.227
	E100	7.152	7.152	24.35	7.152	0.369	0.301	0.095	0.098	0.163
2000	E25	5.908	5.908	31.68	5.908	0.630	0.324	0.096	0.111	0.402
	E50	6.237	6.237	31.24	6.237	0.631	0.347	0.105	0.116	0.389
	E75	6.643	6.643	28.91	6.643	0.569	0.354	0.110	0.114	0.325
	E100	7.152	7.152	27.79	7.152	0.582	0.410	0.130	0.131	0.301
2500	E25	5.908	5.908	18.02	5.908	0.448	0.496	0.167	0.181	0.120
	E50	6.237	6.237	17.58	6.237	0.442	0.507	0.171	0.179	0.106
	E75	6.643	6.643	18.65	6.643	0.474	0.552	0.193	0.190	0.115
	E100	7.152	7.152	18.50	7.152	0.479	0.601	0.211	0.205	0.089

The environmental impact rate related to engine production ($\dot{Y}$) had a constant value of 0.554 mPt/h, considering the environmental impact of the material composition (Table 3) and the weight of the engine, 103 kg.

The specific environmental impact of the fuel (b_2) became higher as the ethanol content increased. Although gasoline has a higher environmental impact per unit of mass (pure gasoline: 264 mPt/kg) than ethanol (214 mPt/kg), the increase in the fuel mass flow rate (Table 4) generated the higher specific environmental impact of fuel (b_2). It must be highlighted that this environmental impact was from "cradle to gate", and did not include combustion (there was a high contribution to the environmental impacts due to the formation of pollutants during combustion).

The specific environmental impact of the exhaust gases (b_3) and exergy losses (b_5) were equal to that of the fuel ($b_f = b_2$), according to the fuel principle within the SPECO methodology.

The specific environmental impact of the brake power (b_4) comprised the environmental impact rates of fuel ($\dot{B}_F$) and pollutant formation ($\dot{B}^{PF}$). As the ethanol content increased, the environmental impact rate of fuel increased, and the environmental impact rate associated with the formation of pollutants decreased.

The low environmental burden of pollutant formation dominated the formation of the specific environmental impacts associated with brake power (b_4) at lower speeds. Hydrous ethanol (E100) had the lowest specific environmental impact (b_4) at 1500 and 2000 rpm. At 2500 rpm, the contribution of the formation of pollutants reduced and the effect of the environmental impact rate of fuel became more significant. The 50% ethanol blend (E50) had the lowest specific environmental impact for the brake power (b_4) at 2500 rpm. Similar performance can be found in the environmental impact rate of the product ($\dot{B}_P$).

The rates of environmental impact related to the exhaust gases ($\dot{B}_3$) and exergy losses ($\dot{B}_L$) increased with higher ethanol contents due to the increase in the specific environmental impact of the fuel (b2) due to its higher mass flow rate of fuel.

Table 6 also shows the average environmental impact rate per exergy unit of the products (power ($\dot{B}_P$) and fuel ($\dot{B}_F$)) of the engine. A reduction in the average environmental impact rate per exergy unit of power ($\dot{B}_P$) occurred due to a reduction in the specific environmental impact of the power produced (b_4), according to Equation (12). Compared with ($\dot{B}_P$), the behavior of the average environmental impact rate per exergy unit of fuel ($\dot{B}_F$) was the opposite: $\dot{B}_F$ increased along with the specific environmental impact of fuel (b_2).

The rate of environmental impacts related to the destruction of exergy ($\dot{B}_D$), also shown in Table 6, showed a slight increase. This resulted from the exergy destruction rate and the specific environmental impact of fuel (b_2). As the ethanol content increased, the exergy destruction rate reduced and the specific environmental impact of fuel increased. The effect of the specific environmental impact of fuel predominated over the exergy destruction rate.

With an increase in ethanol content, there was a general reduction in the environmental impact rate related to the formation of pollutants ($\dot{B}^{PF}$) at all speeds. NOx emissions were the main contributor to the environmental impact rate associated with the formation of pollutants, calculated by multiplying the mass flow rate of NOx by its specific environmental impact per mass of pollutant (b^{PF}_{NO}, 4217.74 mPt/kg). NOx represented approximately 60–90% of the overall environmental impact rate of pollutant formation.

Figure 4 shows the specific environmental impact of brake power for different ethanol contents and engine speeds.

The specific environmental impact of brake power was evaluated by considering reallocation, according to Equation (15). As the ethanol content increased, the environmental impact rate of brake power reduced at low speeds such as 1500 and 2000 rpm. However, this behavior was the opposite at high speeds. The specific environmental impact of brake power comprised the environmental impact rate of the fuel ($\dot{B}_F$), the environmental impact rate of exergy loss ($\dot{B}_{loss}$), and the environmental impact rate of pollutant formation ($\dot{B}^{PF}$). As the ethanol content increased, there was an increase in the environmental impact rates associated with fuel and exergy losses, with a decrease in the environmental impact rate of pollutant formation.

The environmental impact rates of pollutant formation were evaluated by considering each polluting gas and its specific environmental impact per unit of mass (CO_2, CO and NOx) according to Equation (13). Melo et al. [51] tested a SI engine with different mixtures of Brazilian gasoline (25% ethanol by volume) and ethanol, and the progressive addition of ethanol resulted in lower CO and HC emissions, but increased emissions of CO_2.

Figure 5 shows the effect of fuel and environmental impact rates of pollutant formation.

The increase in the environmental impact rate of fuel ($\dot{B}_F$) and the reduction in the environmental impact rate of pollutant formation ($\dot{B}^{PF}$) when the ethanol content increased can be seen in Figure 5.

Figure 6 shows the exergoenvironmental factor (f_b) on the primary *y*-axis (left) and the relative difference in environmental impact (r_b) on the secondary *y*-axis (right).

In Figure 6, the relative difference in the environmental impact (r_b) values decreased as the ethanol content decreased for 2000 and 2500 rpm. For 1500 rpm, r_b increased from

E25 to E50 then decreased for E75 and E100. As r_b represents the environmental quality of a component, the addition of ethanol improves the engine's environmental quality.

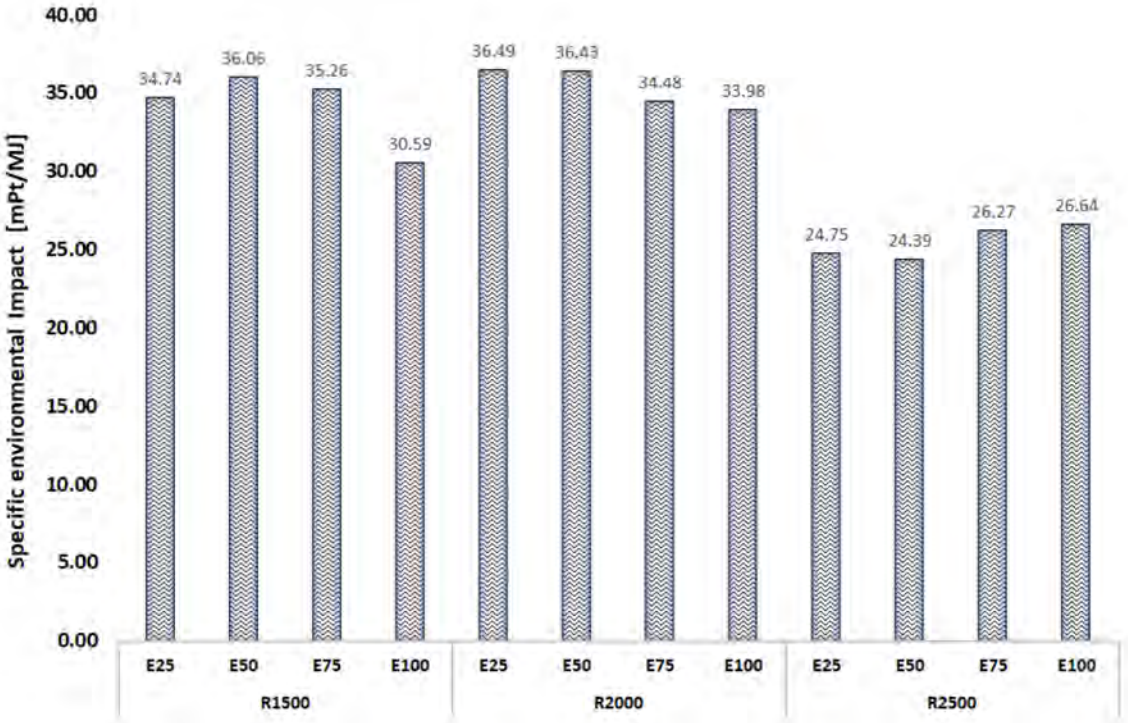

Figure 4. Environmental impact of brake power per exergy unit vs. ethanol contents and engine speeds.

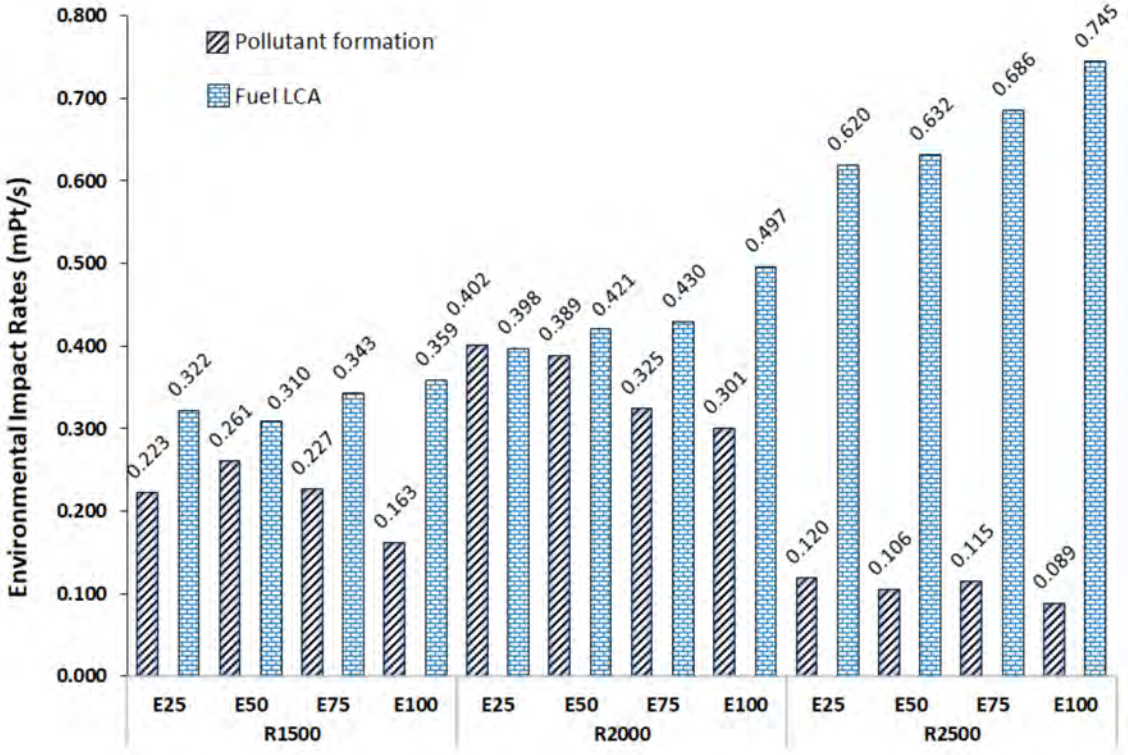

Figure 5. Variation in the environmental impact rates with ethanol content.

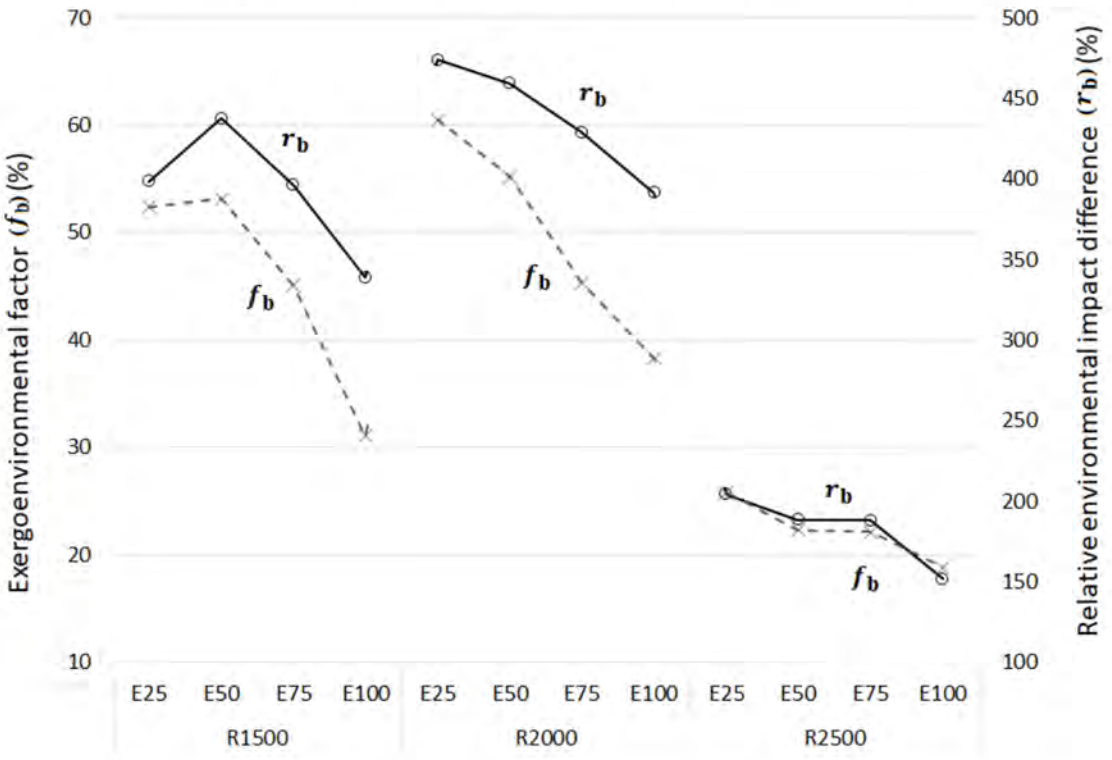

Figure 6. Exergoenvironmental factors and relative differences in environmental impact vs. ethanol content.

The exergoenvironmental factor (f_b) also decreased with increased ethanol content. Pollutant formation should be reduced to improve the environmental performance at 1500 and 2000 rpm. However, at 2500 rpm, the exergy efficiency was lower, which should be increased to reduce the environmental impact rate of exergy destruction and thus improve the environmental performance.

No similar work was found in the scientific literature focusing on an Otto cycle ICE. Cavalcanti et al. [35] carried out an exergoenvironmental analysis of diesel–biodiesel blends in a direct injection engine at variable loads and verified that a higher biodiesel content reduced the environmental impact of fuel and the specific environmental impact of electricity. Figure 7 shows a comparison of the environmental impacts per exergy rate of power: Blend D-B (blends studied by [35]), followed by the ethanol–gasoline blends studied here. Figure 7 presents the ranges of values obtained, where the solid bars denote the lowest value encountered and the dotted bars depict the highest value.

In the work of Cavalcanti et al. [35], diesel–biodiesel blends were studied, ranging from 5 to 100% biodiesel (D95B5 to B100). Pure biodiesel had the lowest environmental impact, 55.8 mPt/kg, while pure diesel had the highest value, 240 mPt/kg. Pure biodiesel produced the lowest specific environmental impact (15.4 mPt/MJ, the lowest value in Figure 7), at the expense of a slight decrease in exergy efficiency from 33.09% (D95B5) to 32.59% (B100). Here, the environmental impacts of ethanol and gasoline were 214 mPt/kg and 264 mPt/kg, respectively, which had the lowest specific environmental impacts in the range of 24.4–26.4 mPt/MJ (solid bars in Figure 7), while the highest were 34.0–36.5 mPt/MJ (dotted bars in Figure 7).

Another critical parameter to consider is the number of yearly operation hours: here, 2200 h/year was considered for the flex engine, while Cavalcanti et al. [35] utilized 4380 h/year for the diesel engine. The higher capacity and weight of the diesel engine (95 kW and 940 kg), compared with the flex engine studied here (77 kW and 103 kg), enabled the longer lifetime of the diesel engine, reducing the environmental impact rate of

the engine. Cavalcanti et al. [35] presented an upper limit of 22.6 mPt/MJ due to the low environmental impact per mass of biodiesel and the higher operation hours of its engine.

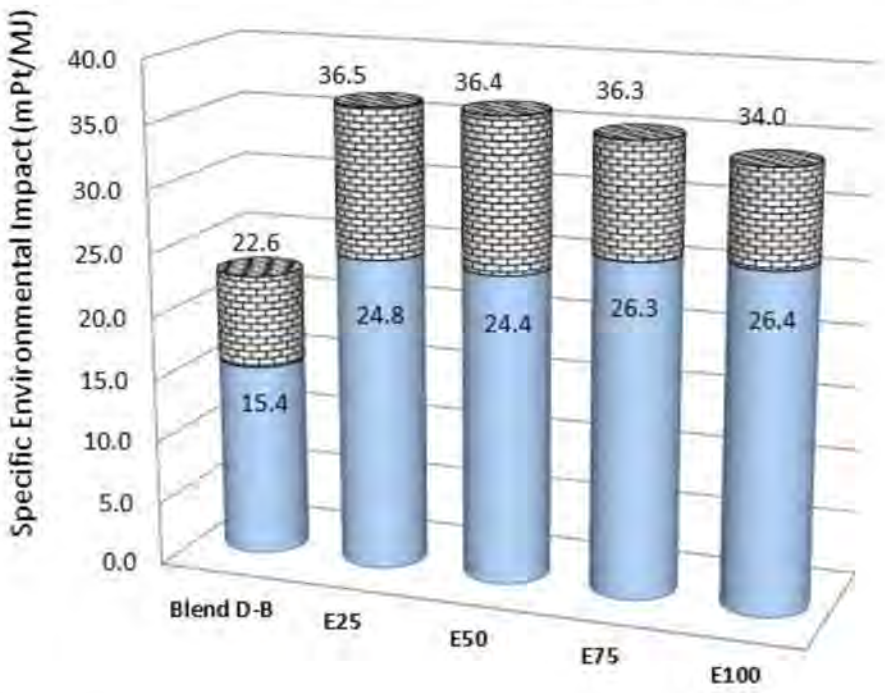

Figure 7. Range of environmental impacts per exergy unit for different fuels and blends.

Cavalcanti [38] reported a gas–diesel marine engine where diesel was replaced by natural gas. Although the efficiency decreased, the emission of pollutants was reduced, reducing the environmental impact of the power rate per exergy unit. The effect of fuel, the environmental rate of pollutant formation, and exergy efficiency should be evaluated for each situation to improve environmental performance.

Different types of bioenergy are currently available and can be integrated within the existing infrastructure, such as the case of ethanol, which was explored here. Going a step further than utilization in ICE, ethanol bioenergy is sufficiently flexible to be redirected to other sectors such as industrial process heat, with the benefits of providing carbon removal from the atmosphere when combined with carbon capture and storage. Brazilian sugarcane ethanol is one of the least carbon-intensive biofuels commercially available, as its production process taps only one-third of the energy the plant can offer (the remainder is contained in leftover fiber and straw) [52]. This means that cellulosic ethanol has the potential to double its yield.

More efforts are required to develop (and deploy) clean energy technologies, which are important for meeting international energy and climate goals, especially regarding the reduction of pollutants associated with transportation. Although the energy transition has slowed down due to the COVID-19 pandemic [53], it must include the power sector and be extended to the transport, industry, and building sectors. According to the International Energy Agency [54], these sectors today account for 55% of carbon emissions from the energy system, and biofuels can be vital solutions. During this transition, ethanol can be a renewable fuel option in ICEs, and the disadvantages can be tackled by adding hydrogen to ethanol, enabling SI engines to achieve lower brake-specific energy consumption, better performance, and lower emissions [55].

However, there is still debate on bioenergy in several countries, and its role in the energy transition is often underestimated [56] despite its importance in moving the global energy system towards carbon neutrality.

Finally, in the aftermath of the COVID-19 pandemic, bioenergy must be incorporated into the recovery plans of the countries, with added benefits such as the promotion of jobs.

Measures to advance the transition through 2030 and beyond, according to the International Renewable Energy Agency [57], include blending mandates for ethanol and biodiesel and offering customized loans for biofuel production. Energy transition and post-pandemic recovery are the following challenges to be faced.

4. Conclusions

From the Life Cycle Assessment, when combustion was not considered, it was verified that the environmental impacts of gasoline and ethanol were not too far apart: 0.264 and 0.214 Pt/kg, respectively. Most of the environmental impacts associated with gasoline production were due to the depletion of resources, while land use dominated the environmental impacts of ethanol.

Exergy and exergoenvironmental analyses were developed for a four-stroke spark-ignition engine with maximum power of 77.2 kW. The engine is fueled with gasoline-ethanol mixtures (25%, 50%, 75% ethanol by volume) and hydrous ethanol (4.6% water by volume) and operates at variable speeds: 1500, 2000, and 2500 rpm. Hydrous ethanol presented the highest CO_2 and CO emissions when combustion was considered. The highest NO_x emissions were obtained for the mixture with 25% ethanol at 2000 rpm.

The highest exergy efficiency (36.93%) was reached with the 75% ethanol blend at 2000 rpm. The highest specific environmental impact related to fuel (b2) was 7.152 mPt/MJ for hydrous ethanol, followed by the 75% ethanol blend with 6.643 mPt/MJ. Although the environmental impact of ethanol is lower than gasoline, the highest environmental impact rate associated with the formation of pollutants was obtained for 25% ethanol blend at 2000 rpm.

The lowest specific environmental impact of product (brake power) was achieved for the 25% ethanol blend at 1500 rpm. This condition presented the best environmental impact performance.

The work presented herein contributes to experience and good practice, and provides scientific evidence of the benefits associated with the utilization of exergoenvironmental assessments to raise awareness of the potential of adding ethanol to gasoline. Future research could focus on deploying this type of bioenergy and scale it up sustainably, connecting it with economic aspects so that its potential does not remain untapped. Other research could be to analyze the engine under conditions of intermediate throttle mode, if performance and emissions data are available.

Author Contributions: Conceptualization, E.J.C.C.; methodology, E.J.C.C. and D.R.S.d.S.; LCA, M.C.; validation, E.J.C.C.; formal analysis, E.J.C.C.; investigation, D.R.S.d.S.; resources, M.C.; data curation, D.R.S.d.S.; writing—original draft preparation, E.J.C.C. and D.R.S.d.S.; writing—review and editing, M.C.; visualization, E.J.C.C. and M.C.; supervision, E.J.C.C. All authors have read and agreed to the published version of the manuscript.

Funding: The authors wish to acknowledge the support of the National Council for Scientific and Technological Development (CNPq, Brazil) Research Productivity grant No. 307394/2018-2. This study was financed in part by the Coordenação de Aperfeiçoamento de Pessoal de Nível Superior-Brasil (CAPES)-Finance Code 001.

Institutional Review Board Statement: Not applicable.

Informed Consent Statement: Not applicable.

Data Availability Statement: Data is available upon request.

Conflicts of Interest: The authors declare no conflict of interest.

References

1. Serrano, J.R.; Novella, R.; Piqueras, P. Why the Development of Internal Combustion Engines Is Still Necessary to Fight against Global Climate Change from the Perspective of Transportation. *Appl. Sci.* **2019**, *9*, 4597. [CrossRef]
2. Anderson, L.G. Effects of using renewable fuels on vehicle emissions. *Renew. Sustain. Energy. Rev.* **2015**, *47*, 162–172. [CrossRef]

3. OICA. International Organization of Motor Vehicle Manufacturers. 2020. Available online: http://www.oica.net (accessed on 5 May 2020).
4. IEA. Data and Statistics—CO_2 Emissions by Sector. World 1990–2017. 2020. Available online: https://www.iea.org/data-and-statistics?country=WORLD&fuel=CO2emissions&indicator=CO2emissionsbysector (accessed on 5 May 2020).
5. Johnsson, F.; Kjärstad, J.; Rootzén, J. The threat to climate change mitigation posed by the abundance of fossil fuels. *Clim. Policy* **2019**, *19*, 258–274. [CrossRef]
6. Awad, O.I.; Mamat, R.; Ali, O.M.; Sidik, N.A.C.; Yusaf, T.; Kadirgama, K.; Kettner, M. Alcohol and ether as alternative fuels in spark ignition engine: A review. *Renew. Sustain. Energy Rev.* **2018**, *82*, 2586–2605. [CrossRef]
7. Shirazi, S.A.; Abdollahipoor, B.; Windom, B.; Reardon, K.F.; Foust, T.D. Effects of blending C3-C4 alcohols on motor gasoline properties and performance of spark ignition engines: A review. *Fuel Process. Technol.* **2020**, *197*, 106194. [CrossRef]
8. Thakur, A.; Kaviti, A.K.; Mehra, R.; Mer, K. Progress in performance analysis of ethanol-gasoline blends on SI engine. *Renew. Sustain. Energy Rev.* **2017**, *69*, 324–340. [CrossRef]
9. Masum, B.; Masjuki, H.; Kalam, A.; Fattah, I.R.; Palash, S.; Abedin, M. Effect of ethanol–gasoline blend on NOx emission in SI engine. *Renew. Sustain. Energy Rev.* **2013**, *24*, 209–222. [CrossRef]
10. Roso, V.R.; Santos, N.D.S.A.; Alvarez, C.E.C.; Filho, F.A.R.; Pujatti, F.J.P.; Valle, R.M. Effects of mixture enleanment in combustion and emission parameters using a flex-fuel engine with ethanol and gasoline. *Appl. Therm. Eng.* **2019**, *153*, 463–472. [CrossRef]
11. Poulopoulos, S.; Samaras, D.; Philippopoulos, C. Regulated and unregulated emissions from an internal combustion engine operating on ethanol-containing fuels. *Atmospheric Environ.* **2001**, *35*, 4399–4406. [CrossRef]
12. He, B.-Q.; Wang, J.-X.; Hao, J.-M.; Yan, X.-G.; Xiao, J.-H. A study on emission characteristics of an EFI engine with ethanol blended gasoline fuels. *Atmospheric Environ.* **2003**, *37*, 949–957. [CrossRef]
13. Zhao, L.; Wang, X.; Wang, D.; Su, X. Investigation of the effects of lean mixtures on combustion and particulate emissions in a DISI engine fueled with bioethanol-gasoline blends. *Fuel* **2020**, *260*, 116096. [CrossRef]
14. Efemwenkiekie, U.; Oyedepo, S.; Idiku, U.; Uguru-Okorie, D.; Kuhe, A. Comparative Analysis of a Four Stroke Spark Ignition Engine Performance Using Local Ethanol and Gasoline Blends. *Procedia Manuf.* **2019**, *35*, 1079–1086. [CrossRef]
15. Iodice, P.; Senatore, A.; Langella, G.; Amoresano, A. Effect of ethanol–gasoline blends on CO and HC emissions in last generation SI engines within the cold-start transient: An experimental investigation. *Appl. Energy* **2016**, *179*, 182–190. [CrossRef]
16. Chen, R.-H.; Chiang, L.-B.; Chen, C.-N.; Lin, T.-H. Cold-start emissions of an SI engine using ethanol–gasoline blended fuel. *Appl. Therm. Eng.* **2011**, *31*, 1463–1467. [CrossRef]
17. da Costa, R.B.R.; Filho, F.A.R.; Coronado, C.J.; Teixeira, A.F.; Netto, N.A.D. Research on hydrous ethanol stratified lean burn combustion in a DI spark-ignition engine. *Appl. Therm. Eng.* **2018**, *139*, 317–324. [CrossRef]
18. Lanzanova, T.D.M.; Nora, M.D.; Zhao, H. Performance and economic analysis of a direct injection spark ignition engine fueled with wet ethanol. *Appl. Energy* **2016**, *169*, 230–239. [CrossRef]
19. da Costa, R.B.R.; Teixeira, A.F.; Filho, F.A.R.; Pujatti, F.J.; Coronado, C.J.; Hernández, J.J.; Lora, E.E.S. Development of a homogeneous charge pre-chamber torch ignition system for an SI engine fuelled with hydrous ethanol. *Appl. Therm. Eng.* **2019**, *152*, 261–274. [CrossRef]
20. Ambrós, W.; Lanzanova, T.; Fagundez, J.; Sari, R.; Pinheiro, D.; Martins, M.; Salau, N. Experimental analysis and modeling of internal combustion engine operating with wet ethanol. *Fuel* **2015**, *158*, 270–278. [CrossRef]
21. Doğan, B.; Erol, D.; Yaman, H.; Kodanli, E. The effect of ethanol-gasoline blends on performance and exhaust emissions of a spark ignition engine through exergy analysis. *Appl. Therm. Eng.* **2017**, *120*, 433–443. [CrossRef]
22. Rufino, C.H.; de Lima, A.J.; Mattos, A.P.; Allah, F.U.; Bernal, J.L.L.; Ferreira, J.V.; Gallo, W.L. Exergetic analysis of a spark ignition engine fuelled with ethanol. *Energy Convers. Manag.* **2019**, *192*, 20–29. [CrossRef]
23. Bhatti, S.; Verma, S.; Tyagi, S. Energy and exergy based performance evaluation of variable compression ratio spark ignition engine based on experimental work. *Therm. Sci. Eng. Prog.* **2019**, *9*, 332–339. [CrossRef]
24. Gharehghani, A.; Hosseini, R.; Mirsalim, M.; Yusaf, T.F. A comparative study on the first and second law analysis and performance characteristics of a spark ignition engine using either natural gas or gasoline. *Fuel* **2015**, *158*, 488–493. [CrossRef]
25. Das, A.K.; Hansdah, D.; Mohapatra, A.K.; Panda, A.K. Energy, exergy and emission analysis on a DI single cylinder diesel engine using pyrolytic waste plastic oil diesel blend. *J. Energy Inst.* **2020**, *93*, 1624–1633. [CrossRef]
26. Hoseinpour, M.; Sadrnia, H.; Tabasizadeh, M.; Ghobadian, B. Energy and exergy analyses of a diesel engine fueled with diesel, biodiesel-diesel blend and gasoline fumigation. *Energy* **2017**, *141*, 2408–2420. [CrossRef]
27. Odibi, C.; Babaie, M.; Zare, A.; Nabi, N.; Bodisco, T.A.; Brown, R.J. Exergy analysis of a diesel engine with waste cooking biodiesel and triacetin. *Energy Convers. Manag.* **2019**, *198*, 111912. [CrossRef]
28. Krishnamoorthi, M.; Sreedhara, S.; Duvvuri, P.P. Experimental, numerical and exergy analyses of a dual fuel combustion engine fuelled with syngas and biodiesel/diesel blends. *Appl. Energy* **2020**, *263*, 114643. [CrossRef]
29. Rakopoulos, D.C.; Rakopoulos, C.D.; Kosmadakis, G.M.; Giakoumis, E.G. Exergy assessment of combustion and EGR and load effects in DI diesel engine using comprehensive two-zone modeling. *Energy* **2020**, *202*, 117685. [CrossRef]
30. Razmara, M.; Bidarvatan, M.; Shahbakhti, M.; Robinett, R. Optimal exergy-based control of internal combustion engines. *Appl. Energy* **2016**, *183*, 1389–1403. [CrossRef]
31. Rakopoulos, C.; Giakoumis, E. Second-law analyses applied to internal combustion engines operation. *Prog. Energy Combust. Sci.* **2006**, *32*, 2–47. [CrossRef]

32. Gude, V.G. Use of exergy tools in renewable energy driven desalination systems. *Therm. Sci. Eng. Prog.* **2018**, *8*, 154–170. [CrossRef]
33. Meyer, L.; Tsatsaronis, G.; Buchgeister, J.; Schebek, L. Exergoenvironmental analysis for evaluation of the environmental impact of energy conversion systems. *Energy* **2009**, *34*, 75–89. [CrossRef]
34. Hamut, H.; Dincer, I.; Naterer, G. Exergoenvironmental analysis of hybrid electric vehicle thermal management systems. *J. Clean. Prod.* **2014**, *67*, 187–196. [CrossRef]
35. Cavalcanti, E.J.; Carvalho, M.; Ochoa, A.A. Exergoeconomic and exergoenvironmental comparison of diesel-biodiesel blends in a direct injection engine at variable loads. *Energy Convers. Manag.* **2019**, *183*, 450–461. [CrossRef]
36. Dogan, B.; Çakmak, A.; Yesilyurt, M.K.; Erol, D. Investigation on 1-heptanol as an oxygenated additive with diesel fuel for compression-ignition engine applications: An approach in terms of energy, exergy, exergoeconomic, enviroeconomic, and sustainability analyses. *Fuel* **2020**, *275*, 117973. [CrossRef]
37. Carvalho, M.A.S. Evaluation of an Otto-Cycle Internal Combustion Engine Using Different Types of Fuels. Master's Thesis, Federal University of Bahia, Salvador, Brazil, 2011. (In Portuguese).
38. Cavalcanti, E.J. Energy, exergy and exergoenvironmental analyses on gas-diesel fuel marine engine used for trigeneration system. *Appl. Therm. Eng.* **2021**, *184*, 116211. [CrossRef]
39. Moran, M.J.; Shapiro, H.N.; Boettner, D.D.; Bailey, M.B. *Fundamentals of Engineering Thermodynamics*; John Wiley & Sons: Hoboken, NJ, USA, 2010.
40. Lazzaretto, A.; Tsatsaronis, G. SPECO: A systematic and general methodology for calculating efficiencies and costs in thermal systems. *Energy* **2006**, *31*, 1257–1289. [CrossRef]
41. Bejan, A.; Tsatsaronis, G.; Moran, M.J. *Thermal Design and Optimization*; John Wiley & Sons: Hoboken, NJ, USA, 1995.
42. Kotas, T.J. (Ed.) Chemical exergy of industrial fuels. In *The Exergy Method of Thermal Plant Analysis*; Butterworth-Heinemann: Oxford, UK, 1985; pp. 267–269. [CrossRef]
43. Kotas, T.J. (Ed.) Chemical exergy and enthalpy of devaluation. In *The Exergy Method of Thermal Plant Analysis*; Butterworth-Heinemann: Oxford, UK, 1985; pp. 236–262. [CrossRef]
44. International Organization for Standardization. *ISO 14040: 2006: Environmental Management—Life Cycle Assessment—Principles and Framework*; ISO: Geneva, Switzerland, 2006.
45. International Organization for Standardization. *ISO 14044: 2006: Environmental Management—Life Cycle Assessment—Requirements and Guidelines*; ISO: Geneva, Switzerland, 2006.
46. Goedkoop, M.; Spriensma, R. *The Eco-Indicador 99: A Damage Oriented Method for Life Cycle Impact Assessment E Methodology Report*, 3rd ed.; Pre Consultants: Amersfoort, The Netherlands, 2001.
47. Goedkoop, M.; Effting, S.; Collignon, M. *The Eco-Indicator 99: A Damage Oriented Method for Life-Cycle Impact Assessment: Manual for Designers*; PRé Consultants: Amersfoort, The Netherlands, 2000.
48. Simapro software. PréConsultants 2020. Available online: https://simapro.com (accessed on 18 April 2020).
49. ECOINVENT. Database 2019. Available online: http://www.ecoinvent.org (accessed on 18 April 2020).
50. Yang, Z.; Wang, B.; Jiao, K. Life cycle assessment of fuel cell, electric and internal combustion engine vehicles under different fuel scenarios and driving mileages in China. *Energy* **2020**, *198*, 117365. [CrossRef]
51. Melo, T.C.C.; Machado, G.B.; Belchior, C.R.; Colaço, M.J.; Barros, J.E.; Oliveira, E.J.; Oliveira, D.G. Hydrous ethanol–gasoline blends–Combustion and emission investigations on a Flex-Fuel engine. *Fuel* **2012**, *97*, 796–804. [CrossRef]
52. Phillips, L. Improving Air Quality Can Help Reduce Fatalities. Ethanol Producer Magazine, August 2020. Available online: http://www.ethanolproducer.com/articles/17421/improving-air-quality-can-help-reduce-fatalities (accessed on 25 November 2020).
53. Carvalho, M.; Delgado, D.B.M.; Lima, K.M.; Cancela, M.C.; Siqueira, C.A.; Souza, D.L.B. Effects of the COVID-19 pandemic on the Brazilian electricity consumption patterns. *Int. J. Energy Res.* **2021**, *45*, 3358–3364. [CrossRef]
54. International Energy Agency. Energy Technology Perspectives 2020—Part of Energy Technology Perspectives. 2020. Available online: https://www.iea.org/reports/energy-technology-perspectives-2020 (accessed on 25 November 2020).
55. Ayad, S.M.; Belchior, C.R.; da Silva, G.L.; Lucena, R.S.; Carreira, E.S.; de Miranda, P.E. Analysis of performance parameters of an ethanol fueled spark ignition engine operating with hydrogen enrichment. *Int. J. Hydrog. Energy* **2020**, *45*, 5588–5606. [CrossRef]
56. Pelkmans, L. Bioenergy Has an Important Role in the Transition Away from Fossil Fuels and to Move the Global Energy System Towards Carbon Neutrality. 2020. Available online: https://www.world-energy.org/article/14052.html (accessed on 25 November 2020).
57. International Renewable Energy Agency (IRENA). *The Post-COVID Recovery: An Agenda for Resilience, Development and Equality*; International Renewable Energy Agency: Abu Dhabi, United Arab Emirates, 2020.